

A Study on Moment Resisting Behavior of Mortise-Tenon Joint with Dowel or Split Wedge

H. Sakata & Y. Yamazaki
Tokyo Institute of Technology, Japan

Y. Ohashi
Tokyo City University, Japan



SUMMARY:

In this paper, moment resisting behavior of mortise-tenon joint with dowel or split wedge is examined. Although mortise-tenon joints are typically used for connection of traditional wooden structures in Japan, their structural characteristics are not evaluated accurately. Bending tests and tension tests are carried out, and performance of the joint with dowel and split wedge are compared. Finally, analytical model to simulate moment resisting behavior is proposed.

Keywords: Timber joint, Mortise-tenon joint, Analysis model, Dowel, Split wedge

1. INTRODUCTION

1.1. Background

Mortise-tenon joints are one of the most typical connections which are used in Japanese traditional timber structure as shown in **Figure 1**. Seismic behavior of timber structure greatly depends on performance of connections, which is not evaluated accurately up to today. Although shear walls basically resist lateral force, timber frame also contributes to seismic performance due to moment resisting of connections. Therefore, we examine moment resisting behavior of mortise-tenon joint with generally-used fasteners which are dowel and split wedge. As shown in **Figure 1**, dowel is used when beam goes through post, and split wedge is used when post goes through beam, respectively.

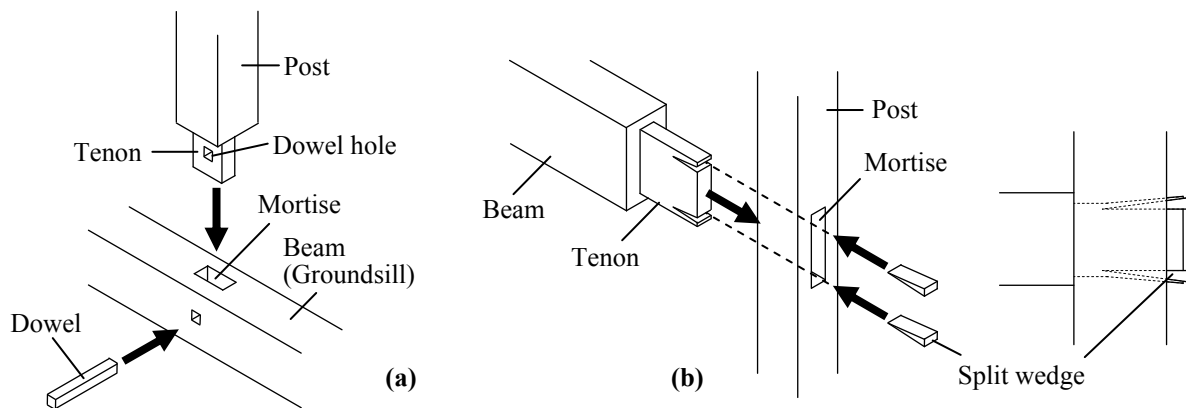


Figure 1: Mortise-tenon joint (a) with dowel (b) with split wedge

1.2. Contents

In Chapter 2, bending tests of joints are carried out. One hundred and eight specimens with dowel and fifty four specimens with split wedge are tested. Bending behavior of joints is discussed by referring to maximum moment, failure mode and envelope curve. In Chapter 3, tension tests of joints are also conducted in order to indentify their basic properties such as material strength. In Chapter 4, cross-section analysis is carried out. Various internal forces are modelled ; local compression forces of timber, friction forces and shear resisting forces of dowel. Moment-rotation relationship is simulated by solving equations of equilibrium and using compatibility conditions. Comparison between test results and analytical results are presented, which shows good agreement. In Chapter 6, the findings of this research are summarized.

2. BENDING TESTS

2.1. Specimen

Specimens are shown in **Figures 2 and 3**. Post and beam are connected each other with mortise and tenon, and fasteners are dowel or split wedge. Dowel is inserted into a hole in order to prevent post from uplifting. As for split wedge, front edge of tenon is preliminary split, and split wedge is inserted to the crack. By doing so, connection is fixed.

List of specimens is shown in **Tables 1 and 2**. Their parameters are dimension of tenon, post, beam and dowel and also tree species of members. Six specimens per one specification were tested. Material properties are shown in **Table 3**. Oak is used for dowel and split wedge, and its average specific gravity was 0.88.

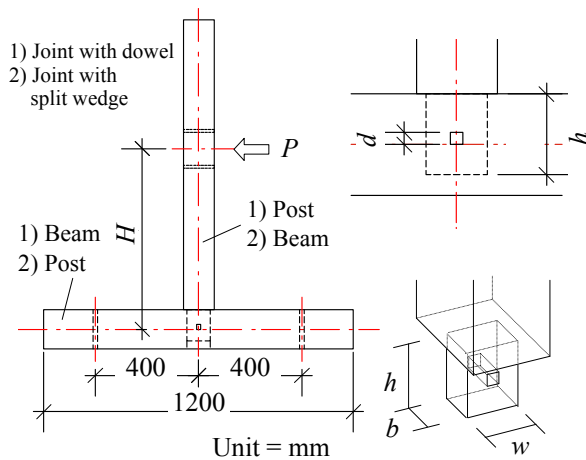


Figure 2: Specimen of bending tests

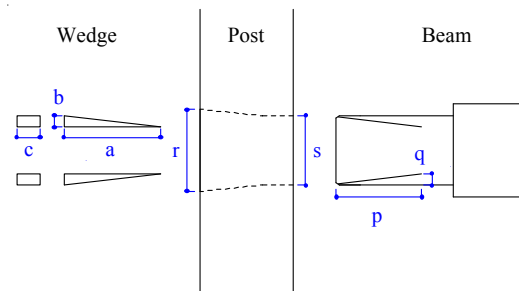


Figure 3: Dimension of joint with split wedge

Table 1: List of Specimens of bending test (with dowel) Unit = mm

Name	Post section	Beam section	Tenon	Dowel section	Number of specimens
			Length×Width×Thickness		
BD-No.1	120×120	120×120	120×90×30	15×15	6
BD-No.2	150×150	150×150	150×120×36	18×18	
BD-No.3	120×120	120×150	120×90×30		
BD-No.4			150×90×30		
BD-No.5			120×90×36		
BD-No.6			150×90×36		

Three combination of tree species were tested;

(i) Post = C, Beam = C (CC) (ii) Post = C, Beam = H (CH) (iii) Post = H, Beam = H (HH)
C = Cedar , H = Hinoki cypress

Table 2: List of specimens of bending test (with split wedge)

Name	Post section	Beam section	Tenon	Wedge dimension	Saw split		Mortise		Number of specimens
			Length×Width×Thickness	a×b×c	(p)	(q)	(r)	(s)	
BS-No.1	120×120	120×120	150×90×30	125×15×30	110	15	105	90	6
BS-No.2	150×150	150×150	180×120×36	145×18×36	125	18	140	120	
BS-No.3	180×180	180×180	210×150×36	160×20×36	150	20	180	150	
BS-No.4	120×120	120×120	150×90×36	125×15×36	110	15	105	90	

Three combinations of tree species were tested. (See **Table 1**)

Table 3: Material properties (Specimens of bending test)

Tree species	Specific gravity (-)	Moisture content (%)	Young's modulus (kN/mm ²)	Bending strength (N/mm ²)	(a): Joint with Dowel
Cedar (C)	0.48	15.7	6.19	39.20	
Hinoki cypress (H)	0.58	14.8	9.47	58.37	

Tree species	Specific gravity (-)	Moisture content (%)	Young's modulus (kN/mm ²)	Bending strength (N/mm ²)	(b): Joint with Split wedge
Cedar (C)	0.41	10.2	6.51	42.87	
Hinoki cypress (H)	0.51	9.4	8.84	60.01	

2.2. Setup and loading schedule

Setup of bending test is shown in **Figure 4**. In the case of joints with dowel (split wedge), beam (post) was fixed to steel foundation beam with anchor bolts. Lateral force was applied to loading point of post (beam) by actuator. Let γ be drift angle of post (beam), and it is calculated using following equation.

$$\gamma = \left(\frac{u_1 + u_2}{2} - \frac{u_3 + u_4}{2} \right) / H \quad (2.1)$$

Where, u_1, u_2 = lateral displacement of loading point, and u_3, u_4 = those of beam (post). H is the distance between center axis of beam (post) and loading point, which was set 700 mm. In the case of joints with split wedge, post is replaced with beam. In other words, specimen is rotated 90 degrees.

Loading schedule is controlled by γ , and static reverse cyclic loading is applied. In addition, relative rotation angle, uplift and shear sliding between post and beam are also measured.

2.3. Test results

2.3.1. Hysteresis and failure mode

Let M and θ be moment and relative rotation angle at joint surface, respectively, which are shown in **Figure 5**. An example of M - θ hysteresis of joint with dowel (BD-No.5(CC)) and split wedge (BS-No.4(CC)) are shown in **Figures 6** and **7**. Their hystereses were very similar, and moment did not decrease even in large deformation such as 1/15 rad. As for joint with dowel, two failure modes were typically observed as shown in **Picture 1**; one was shear failure of tenon from dowel's hole to end, and another was bending failure of tenon around critical section at the side where tensile stress were applied. Failure of dowel was rare case at a rate of about three in one hundred and eight. In the case of joint with split wedge, bending failure of tenon was frequently observed (**Picture 2**). It is noted that preliminary splits might be expanded by inserting wedges.

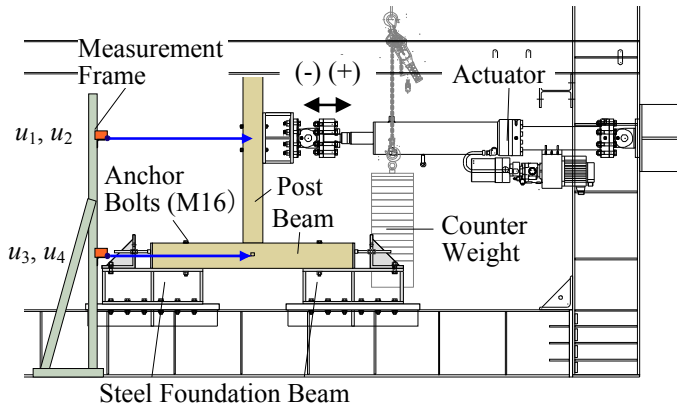
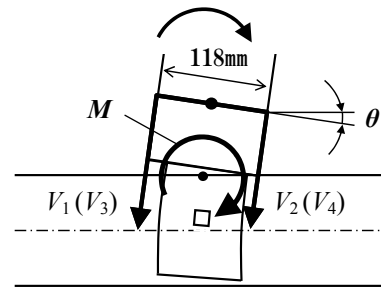


Figure 4: Setup of bending tests



M = Moment at joint surface
 θ = Relative rotation between post and beam

Figure 5: Measurement

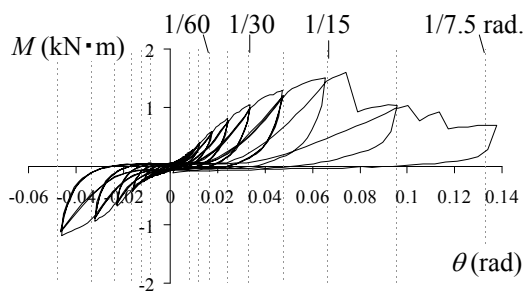
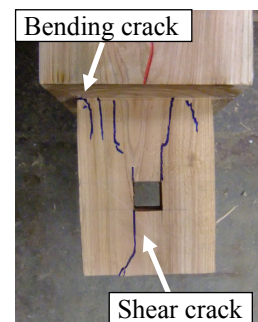


Figure 6: Hysteresis of M - θ relationship
 (An example of BD-No.5(CC))



Picture 1: Observed failure mode
 (Joint with dowel)

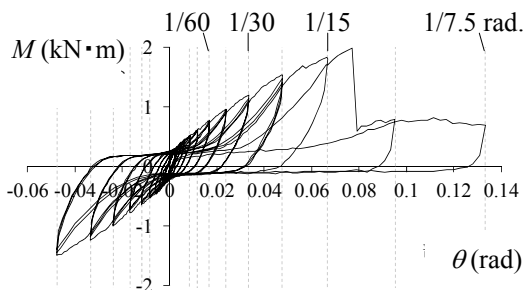
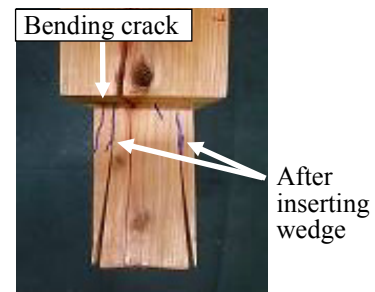


Figure 7: Hysteresis of M - θ relationship
 (An example of BS-No.4(CC))



Picture 2: Observed failure mode
 (Joint with split wedge)

2.3.2. Envelope curve

Envelope curves of M - θ relationship of joint with dowel (BD-No.5(CC)) and joint with split wedge (BS-No.4(CC)) are shown in **Figure 8**. Average curve and standard deviation are also presented in the figure. Maximum moment of the two types of joints were not so different except for one specimen because bending strength was determined by bending failure of tenon, which had no relationship to fasteners. As for split wedge, initial stiffness was increased and variability in stiffness was decreased compared to dowel.

2.3.3. Comparison of maximum moment of two types of joints

Maximum moment M_{max} of two joints are summarized in **Table 4**. Specimens having the same section of tenon are compared in order to discuss the effect of fasteners. In the case of CC, two types

of joints seem to have nearly the same M_{\max} . However, in the case of HH, M_{\max} of split wedge were a little larger than those of dowel.

3. TENSION TESTS

3.1. Specimen and test method

As described in Section 2.3, shear failure of tenon from dowel's hole to end was often observed. Therefore, tension tests were carried out in order to identify shear strength of tenon. In this test, wooden dowel was replaced by steel dowel so that shear failure could certainly happen. Material properties of specimens of tension test are shown in **Table 5**. List of specimens is shown in **Table 6** and **Figure 9**, and setup of tension test is shown in **Figure 10**. Tension force was applied to post and relative displacement was measured between post and steel dowel.

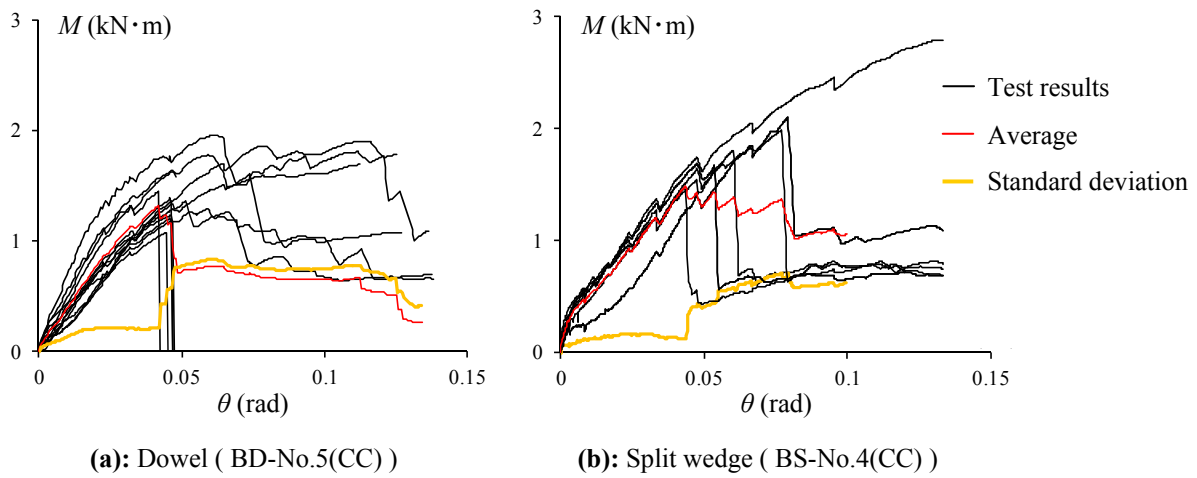


Figure 8: Envelope curve of M - θ relationship

Table 4: Comparison of M_{\max} between split wedge and dowel

	Tree species	Average of M_{\max}	
		Split wedge	dowel
$h = 120$	CC	1.69	1.67
$b = 30$	HH	2.29	1.98
$h = 120$	CC	1.97	2.18
$b = 36$	HH	3.2	2.19

Table 5: Material properties (Specimens of tension test)

Tree species	Specific gravity (-)	Moisture content (%)
Cedar (C)	0.41	13.1
Hinoki cypress (H)	0.51	11.1

Table 6: List of specimens of tension test (Joint with dowel)

Name	Post section	Tenon height (h)	Tenon thickness (b)	Tenon width (w)	End distance (e)	Number of specimens
T-No.2	150×150	150	36	120	75	6
T-No.3	120×120	120	30	90	45	
T-No.4		150			75	
T-No.5		120	36	45		
T-No.6		150		75		

Two cases of tree species (Cedar and Hinoki cypress) were tested.

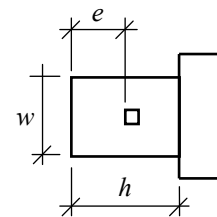


Figure 9: Dimension of tenon

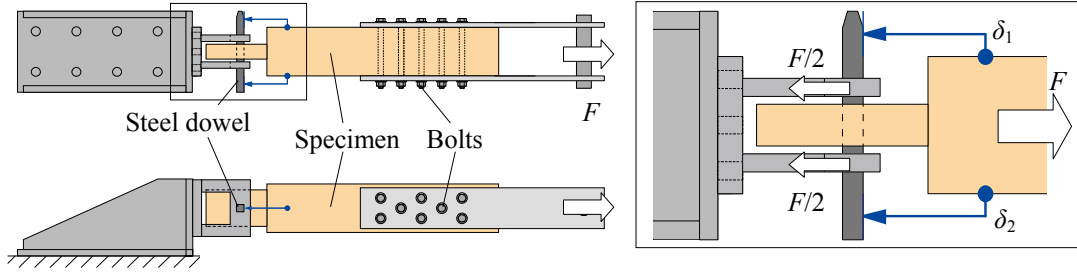


Figure 10: Setup of tension test of mortise-tenon joint with steel dowel

3.2. Test result

Relationship between tension force F and deformation δ is shown in **Figure 11**. Both ductile failure and brittle failure were observed. Standard shear strength are calculated from test results, which mean 95% lower limit of 75% confidence level. They are commonly used in design of timber structure in Japan, and compared to values listed in design code of Japan in **Table 7**. Because they do not appear to be so different, shear strength value of design code can be applied in this case.

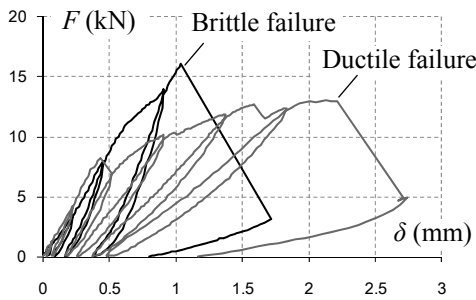


Figure 11: F - δ relationship

Table 7: Shear strength obtained from tension test

Tree species		Cedar	Hinoki cypress
Average (N/mm^2)		2.18	2.85
Number of specimens		30	30
Standard deviation (N/mm^2)		0.6	0.84
Coefficient of variation		0.3	0.29
Standard shear strength (*)	Test result $F_{s,exp}$ (N/mm^2)	1.61	2.3
	Design code F_s (N/mm^2)	1.8	2.1

(*) 95% lower limit of 75% confidence level

4. CROSS-SECTION ANALYSIS

4.1. Analysis model

Figure 12 shows equilibrium condition between external forces and internal forces. External forces consist of axial force N , shear force Q and moment M , and following four kinds of internal forces are considered.

F_{cx1} and F_{cx2} are local compression forces of tenon against beam (post). Index “1” shows force on the end of tenon, and “2” shows that on its root. F_{cy} shows local compression force of post (beam) against beam (post). F_{fy1} and F_{fy2} are friction forces which occur between tenon and mortise. In the case of joint with dowel, resisting forces of dowel F_{dx} and F_{dy} are considered. Index “x” and “y” show forces along x- and y-direction, respectively.

Tenon is assumed to be rigid and to rotate around neutral axis. The original is set in center and root of tenon, and let x_n and y_n be distances from the original to neutral axes.

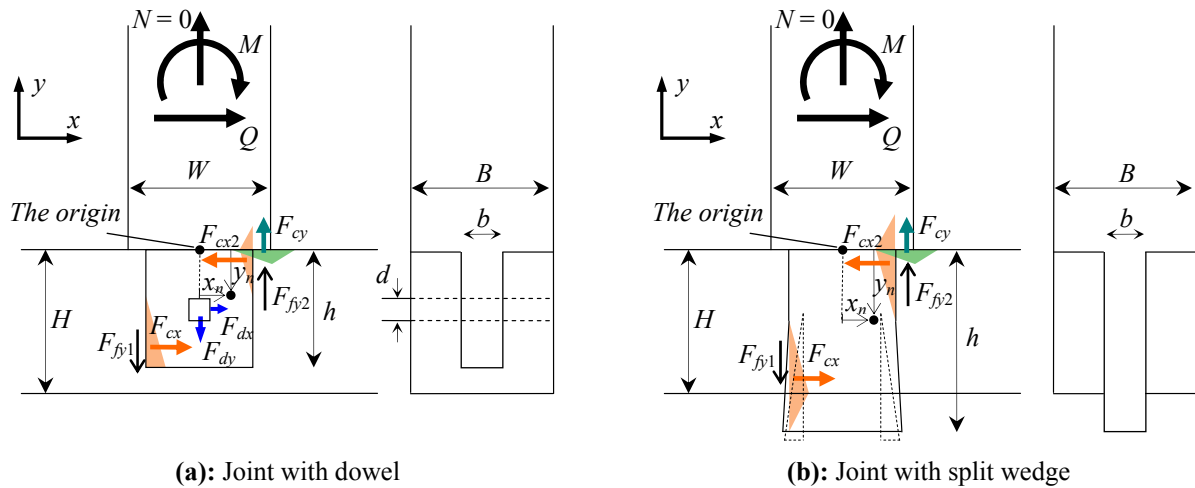
4.2. Local compression forces of timber

When rotation occurs in connection, we can assume triangular compressions of timber perpendicular to the grain. In this paper, such triangular compressions are described as “rotational compressions”. We conducted rotational compression test of timber as shown in **Figure 13** (Sakata et al. 2002). We

found that yield stress could apparently increase in the case of rotational compression compared to translational compression. This is because when maximum edge stress reaches σ_{y0} , surrounding timber is likely to keep elastic and delay yielding. Based on the results of rotational compression tests, we found out $E_1 = E_{10}$, $E_2 = E_{20}$ and $\sigma_y = 1.5\sigma_{y0}$ should be used for calculating local compression forces. Where, E_{10} = elastic Young's modulus, E_{20} = plastic Young's modulus and σ_{y0} = yield stress of translational compression, which are obtained by approximating its stress-strain curve to bi-linear model (Sakata et al. 2006). E_1 , E_2 and σ_y are those of rotational compression. **Table 8** shows results obtained from translational compression tests, which lists maximum, average and minimum values for each tree species.

Moreover, the effect of surplus length of timber must be considered when it is compressed partially, and the effect can be simply evaluated as shown in **Figure 14**. In other words, triangular strain spreads to surplus timber in a half length of contact surface (Sakata et al. 2002, 2006).

Based on above assumption, F_{cx1} , F_{cx2} and F_{cy} are mathematically obtained using only geometric parameters (tenon length, width and thickness and so on) and material properties (Young's modulus and yield stress). In this paper, material properties are obtained from compression test perpendicular to the grain as shown in **Table 8**.



External forces

N : Axial force, Q : Shear force, M : Moment (In this test, $N = 0$)

Internal force

F_{cx1} , F_{cx2} : Local compression forces of tenon against beam (post)

F_{cy} : Local compression force of post (beam) against beam (post)

F_{fy1} , F_{fy2} : Friction forces (F_{fy1} and F_{fy2} are proportional to F_{cx1} and F_{cx2} , respectively.)

F_{dx} , F_{dy} : Resisting forces of dowel in x - and y - direction, respectively (in the case of joint with dowel)

Neutral Axis

x_n , y_n : The distances from the original to neutral axes

Figure 12: External forces and internal forces

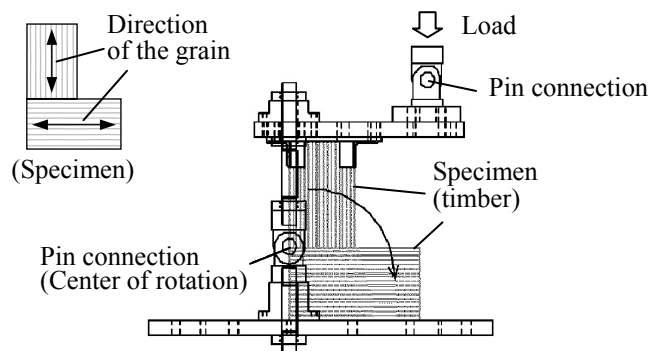


Figure 13: Rotational local compression test (Sakata et al. 2002)

Table 8: Test results of translational compression perpendicular to the grain

(a): Joint with dowel

Tree species		Elastic Young's modulus E_{10} [N/mm ²]	Plastic Young's modulus E_{20} [N/mm ²]	Yield stress σ_{y0} [N/mm ²]
Hinoki cypress	max	327.6	6.30	3.80
	ave	298.7	4.20	3.30
	min	243.9	2.40	3.10
Cedar	max	356.9	7.72	3.41
	ave	279.2	5.07	2.89
	min	215.2	2.34	2.51

(b): Joint with split wedge

Tree species		Elastic Young's modulus E_{10} [N/mm ²]	Plastic Young's modulus E_{20} [N/mm ²]	Yield stress σ_{y0} [N/mm ²]
Hinoki cypress	max	677.7	11.61	7.77
	ave	456.7	8.92	4.98
	min	391.8	5.51	4.12
Cedar	max	370.7	10.09	3.65
	ave	275.9	5.61	3.37
	min	192.8	1.86	3.00

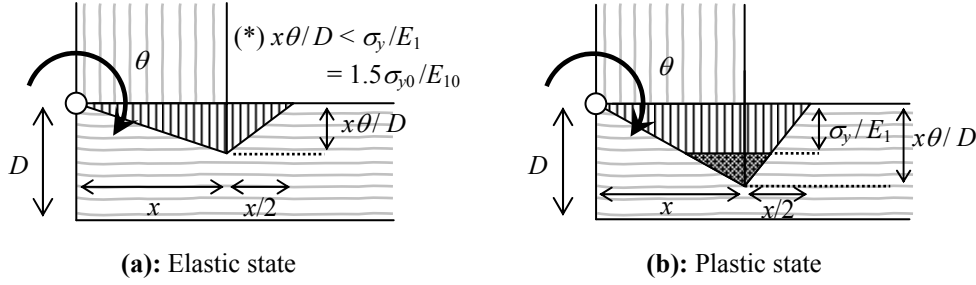


Figure 14: Considering model of strain distribution

4.3. Friction forces

We assume friction forces F_{fy1} and F_{fy2} can be modelled on coulomb friction, and F_{cx1} and F_{cx2} are their normal forces. F_{fy1} and F_{fy2} are calculated as follows.

$$F_{fy1} = \mu F_{cx1} \quad , \quad F_{fy2} = \mu F_{cx2} \quad (4.1a,b)$$

Where, μ = coefficient of friction. In order to take into account variability of test result, we use both coefficient of dynamic friction and static friction. As for dynamic friction, $\mu = 0.17$ is used for CC (only Cedar), $\mu = 0.22$ for HH (only Hinoki cypress), and $\mu = 0.2$ for CH (Cedar and Hinoki cypress) respectively referring to Wood Industry Handbook. As for static friction, $\mu = 0.54$ is used regardless of tree species.

4.4. Resisting forces of dowel

In the case of joint with dowel, it resists slip between tenon and beam, and its force is modelled on “double shear joint with wooden dowel” by referring to design manual for engineered timber joint (in Japanese). Let Δx and Δy be slips in center of dowel in x - and y -direction, respectively. In addition, K_{dx} and K_{dy} are initial stiffness, and $F_{dx,y}$ and $F_{dy,y}$ are yield forces of dowel when only shear force is applied in x - and y -direction, respectively. F_{dx} and F_{dy} are calculated as follows.

$$F_{dx} = K_{dx} \Delta x \quad (\Delta x < F_{dx,y} / K_{dx}) \quad , \quad F_{dy} = K_{dy} \Delta y \quad (\Delta y < F_{dy,y} / K_{dy})$$

$$= F_{dx,y} \quad (\Delta x \geq F_{dx,y} / K_{dx}) \quad , \quad = F_{dy,y} \quad (\Delta y \geq F_{dy,y} / K_{dy}) \quad (4.2a,b)$$

$$\Delta x = (d/2 - y_n) \theta \quad , \quad \Delta y = x_n \theta \quad (4.3a,b)$$

Shear force-slip relationship in each direction are modelled on elasto-perfectly plastic type as shown in Eqns. (4.2a) and (4.2b). Evaluation formulae for K_{dx} , K_{dy} , $F_{dx,y}$ and $F_{dy,y}$ are omitted in this paper. However, ductility of dowel resisting is quite variable as shown in **Figure 11**. Therefore, analytical result after yielding of dowel resisting may have less reliability. It is noted that resisting force of dowel is omitted in the case of joint with split wedge.

4.5. Equations of equilibrium

At first, arbitrary θ is applied, and three equations of equilibrium are expressed using supposed x_n , y_n and Q as follows.

$$\begin{aligned} F_{cx1} - F_{cx2} - F_{dx} + Q = 0 \quad , \quad -F_{cy} + F_{fy1} - F_{fy2} + F_{dy} = 0 \\ M_{cx1} + M_{cx2} + M_{cy} + F_{fx1}(w/2 - x_n) + F_{fx2}(w/2 + x_n) + F_{dx}y_n + F_{dy}x_n - Q(L - H/2 + y_n) \end{aligned} \quad (4.4a-c)$$

(In the case of joint with split wedge, F_{dx} and F_{dy} are removed.)

Where, M_{cx1} , M_{cx2} and M_{cy} = moment at center of rotation caused by F_{cx1} , F_{cx2} and F_{cy} , respectively. Eqns. (4.4) show equilibrium of x -direction, y -direction and around center of rotation, respectively. It is noted that moment at joint surface which is defined in bending test is express by $M = Q(L - H/2)$.

By solving Eqns. (4.4), which require convergent calculation, three unknowns, x_n , y_n and Q are decided. Repeating above calculation with gradually increased θ leads to getting M - θ relationship of connection.

5. COMPARISON BETWEEN TEST RESULTS AND ANALYTICAL RESULTS

Accuracy of analytical method is confirmed. **Figures 15 and 16** show comparisons between test results and analytical results of M - θ relationship. After yielding of dowel resisting (shear failure), bold lines of analytical results are replaced by dash lines. In order to take into account variability of test result, two cases of analysis were conducted. One is using maximum value of material test (**Table 8**) and coefficient of static friction. Another is using minimum value of material test and coefficient of dynamic friction. They are corresponding to upper limit and lower limit of analytical results. Analytical results give good agreement with test results until the failure points, and variability of test results are also simulated. In addition, failure point seems to be predicted by bending strength of tenon which is product of section modulus and material strength of tenon or by yielding point of dowel resisting in the case of joint with dowel.

6. CONCLUSIONS

In this paper, bending tests of mortise-tenon joint with dowel or split wedge were conducted, and its M - θ relationship, failure mode and the effect of tree species and dimension of tenon on maximum moment were shown. After that, evaluation method of M - θ relationship based on constitutive law of rotational compression which we had found out was proposed, and its applicability was shown. Analytical results gave close agreement with test results until the failure point.

AKNOWLEDGEMENT

This bending test is part of “Test Project for Seismic Performance Verification of Japanese Traditional Wooden Houses” which is conducted by “Incorporated association, Kiwoikasu Kenchikusuishin Kyogikai (in Japanese)” with support from Ministry of Land, Infrastructure, Transport and Tourism. We would like to express our gratitude to them. In addition, a number of bending tests were carried out with help from our graduate students. Special thanks to Mr. Udagawa and Mr. Noguchi.

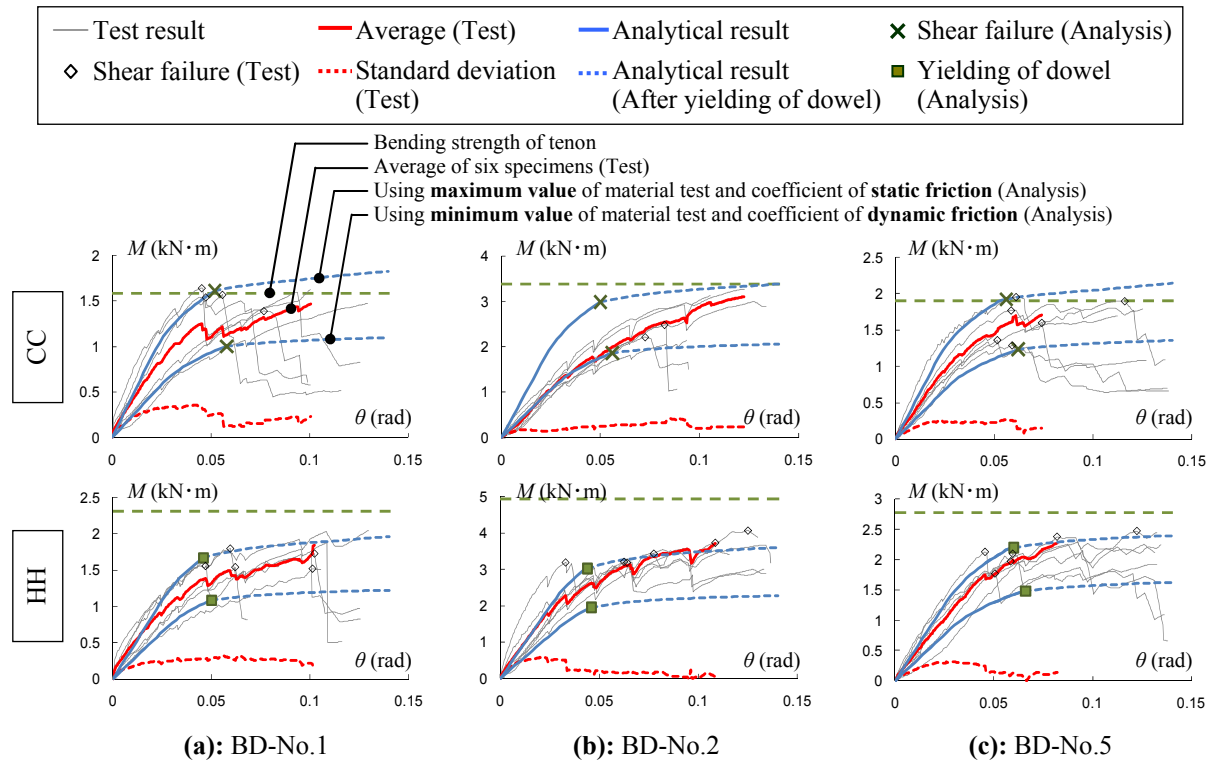


Figure 15: Comparison between test results and analytical results (Joint with dowel)

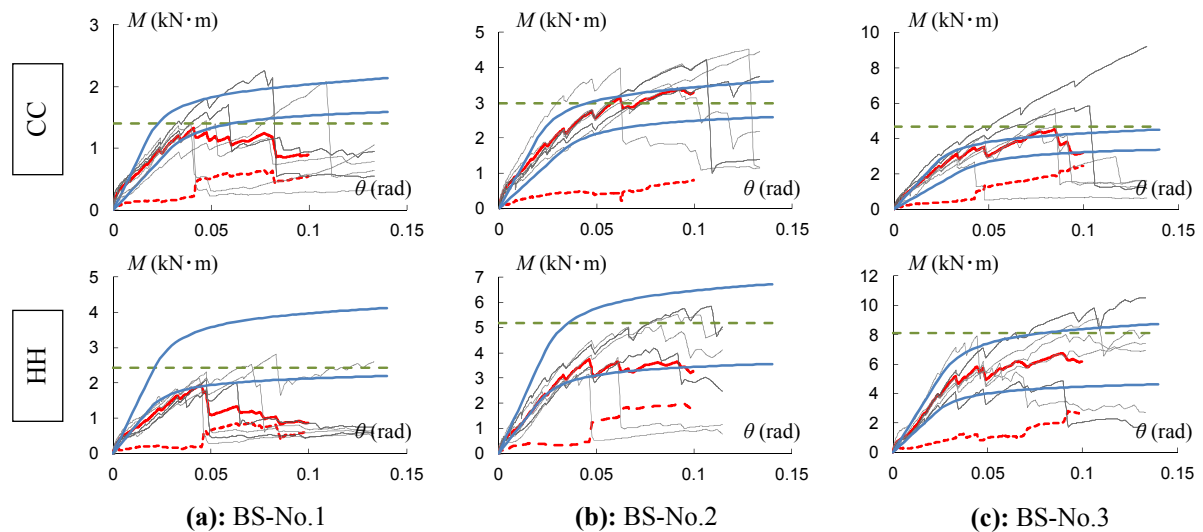


Figure 16: Comparison between test results and analytical results (Joint with split wedge)

REFERENCES

- Architectural Institute of Japan, Design Manual for Engineered Timber Joints, 102-104.
- Matsubara, Y., Du, Z., Sakata, H., Wada, A., Ito, H. and Kataoka, R. (2002) : Experimental Study on the Behavior of Rotational Embedment between Douglas Fir Glulams, *Summaries of technical papers of Annual Meeting Architectural Institute of Japan*, C-1, 27-28.
- Sakaguchi Y., Sakata H., Nakata K., Nakano T., Ito H. and Kataoka R. (2006) : Experimental Study on Mechanical Behavior of Timber Semi-Rigid Joint using Hanger with Drift Pins Part2. M-θ Estimation Method, *Summaries of technical papers of Annual Meeting Architectural Institute of Japan*, C-1, 127-128.
- Forestry and Forest Products Research Institute (2004), *Wood Industry Handbook*, Maruzen, Vol 4, 128-129.